JOURNAL OF MATERIALS SCIENCE 31 (1996) 2227–2240

Structure–properties relationships in rotationally moulded polyethylene

M. J. OLIVEIRA, M. C. CRAMEZ
Departamento de Engenharia de Polímeros, Universidade do Minho, Guimarães, Portugal
R. J. CRAWFORD*
School of Mechanical Engineering, Ashby Building, Queen's University, Belfast BT9 5AH, Northern Ireland

The relationship between structure and properties of rotationally moulded polyethylene was studied using three different contents of antioxidant – 0.04% (standard), 0.1% and 1% – and two different mould atmospheres – air and nitrogen. The mechanical behaviour of the moulded parts was interpreted in terms of the structure of the polymer and the level of degradation at the inner surface of the mouldings. The degree of degradation was assessed using Fourier transform–infrared spectroscopy, fluorescence microscopy and melt-flow index measurements. The microstructure was observed using polarized light microscopy and scanning electron microscopy. The mechanical strength was evaluated by impact testing using an instrumented drop weight machine. The results showed that as the maximum temperature of the gas inside the moulding increases, the impact strength also increases, reaching a maximum at about 225 °C. This build up in impact strength is related to the improved sintering of the plastic powder/melt with time and temperature. However, as is well known in the industry, the moulding conditions needed to achieve optimum properties are critical because a small amount of overheating causes the impact strength, for example, to decrease dramatically. This decrease is due to the degradation that occurs at the inner surface of the samples. This occurs because the surface is in contact with oxygen during processing, leading to oxidation reactions in the material, predominantly resulting in cross-linking. The cross-linked material is responsible for the low impact strength and for the brittle behaviour of samples moulded at higher temperatures. The morphology of these samples is not characterized by the polyethylene spherulitic texture, observed across the thickness of the samples moulded at lower temperatures. The morphology at the inside surface was modified and gave rise to a thin layer of very small and imperfect spherulites, which disappear when the heating is too severe. Next to it is a columnar-type structure made of bundles of parallel fibrils. The increase of antioxidant content and the use of a nitrogen atmosphere caused a delay of the degradation process, but did not prevent it. No significant mechanical strength improvements were observed in these conditions, but a broader processing window was available.

1. Introduction

It is well known that one of the major attractions with plastics is the wide range of manufacturing methods which are available. This gives the designer many options to create simple or complex shapes at an economic rate using plastics selected from the many hundreds of different grades and types of material which are available.

The major processing methods for plastics are injection moulding and extrusion but in certain circumstances these may restrict the designer – for example, in terms of the shapes that can be produced or in terms of the numbers of products required. It is important, therefore, to have available other manufacturing techniques, such as thermoforming or rotational moulding, to fill the gaps. This paper is concerned with rotational moulding and, in particular, with the interrelationships between the microstructure and morphology which arise as a result of processing and the mechanical properties of the end-product.

Although rotational moulding is generally regarded as one of the minor processing methods for plastics, over the past 20 years there have been determined efforts to improve the technology of the process [1–7]. This work has been necessary because rotational moulding emerged from very humble beginnings as

*Author to whom all correspondence should be addressed.

0022–2461

a slow method for manufacturing hollow toys. For many years its growth was hampered by a lack of plastics suitable for the process. There were few advances in terms of machinery controls or mould design and so expansion of the process relied heavily on the skills of the moulder to create imaginative shapes which met the market need at an attractive price. However, within the past decade there has been a major transformation in the industry – new types of machine control have taken the trial and error out of the process, new plastics have been developed for rotomoulding and new mould designs are emerging [7–12]. Nowadays, rotational moulding is one of the fastest growing sectors of the polymer processing industry. Its annual growth rate is about 12% and to sustain this expansion, it is essential to have the technical back-up to ensure that manufacturing is optimized in terms of product quality and cycle times.

As with all processing methods for plastics, designers employing rotational moulding need to take into account a number of key factors such as the influence which the processing conditions have on the properties of the moulded article. As will be shown in the following section, rotational moulding is quite different to other melt processes such as injection moulding or extrusion. For example, with rotomoulding, the heating and cooling rates utilized can cover a wide range and so a much broader spectrum of structural morphologies can be created. Also, only one surface of the plastic product is in contact with the metal mould. The other free surface will normally experience a different cooling rate and may also be subjected to thermal or oxidative degradation. The microstructure of rotationally moulded products is unique and yet it has never been studied in detail and has never been related to the mechanical properties of the mouldings. This paper will attempt to describe the nature of the microstructure in rotomoulded articles, the manner in which this is controlled by processing conditions and the effects which the structure has on the performance of the end-product. The majority (approximately 90%) of rotationally moulded products are made from polyethylene and so this paper concentrates on the microstructure of a typical rotational moulding grade.

2. Nature of the process

Although rotationally moulded products can have a wide variety of shapes and sizes, the easiest way to visualize how the process works is to consider it as a means of making hollow plastic articles. The important stages in the process are illustrated in Fig. 1. It may be seen that from the outset, rotational moulding is quite different from other processing methods for plastics. At the beginning of the cycle, plastic powder (or liquid) is placed in an open, shell-like metal mould. Both the plastic and the mould are at room temperature.

The mould is then closed and clamped. It progresses into an oven and is heated whilst it is rotated about two perpendicular axes so as to distribute the plastic in some desired fashion over the inside surface of the mould. Occasionally other methods of heating may be used, e.g. rotating the mould over an open flame. However, the vast majority of modern commercial machines use a gas-fired oven to heat the plastic.

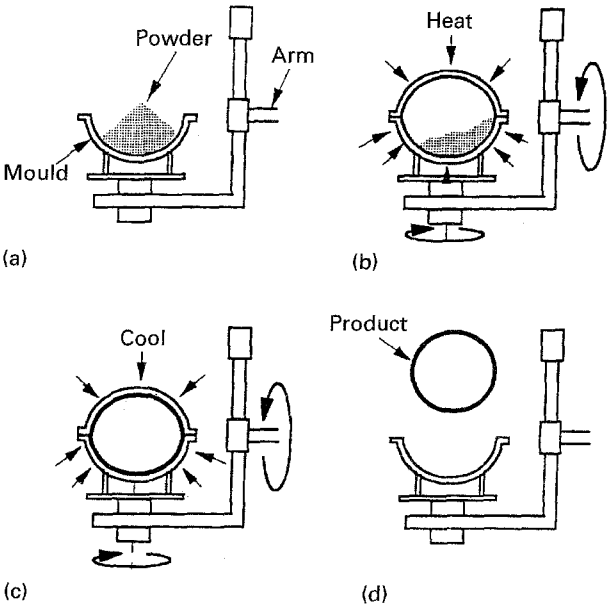

Figure 1 Principles of rotational moulding: (a) mould charging, (b) mould rotation and heating, (c) mould rotation and coding, (d) de-moulding.

The speed of rotation is relatively slow, typically about 10 r.p.m. and the speeds about each axis are usually different in order to ensure the required distribution of the plastic [10]. Once all the plastic has melted and formed the desired coating on the inside of the mould, the biaxial rotation continues as the mould progresses into a cooling bay. Here, forced air or water mist or water spray are directed at the mould in order to cause the plastic to solidify. Still or forced air cause the slowest cooling rate and are generally used in the initial stages of the cooling so as to avoid warpage of the moulding and create a strong product. Once the plastic has solidified the cooling rate can be increased using a water spray so that the mould returns to room temperature for product ejection.

Although rotational moulding has the disadvantage of being a relatively slow processing method, it has a number of very significant advantages which make it attractive to the designer. For example, the moulds are relatively inexpensive and so complex, large products can be manufactured economically in short production runs. Also, there is no stress on the plastic as it is being processed so that the end-products contain little or no residual stresses.

3. Anatomy of the rotational moulding cycle

From the foregoing section it might appear that rotational moulding is a very simple processing method. It might also appear that there is little scope for technical innovation. Both of these assumptions would be wrong because rotational moulding is a complex process which in the past has relied heavily on trial and

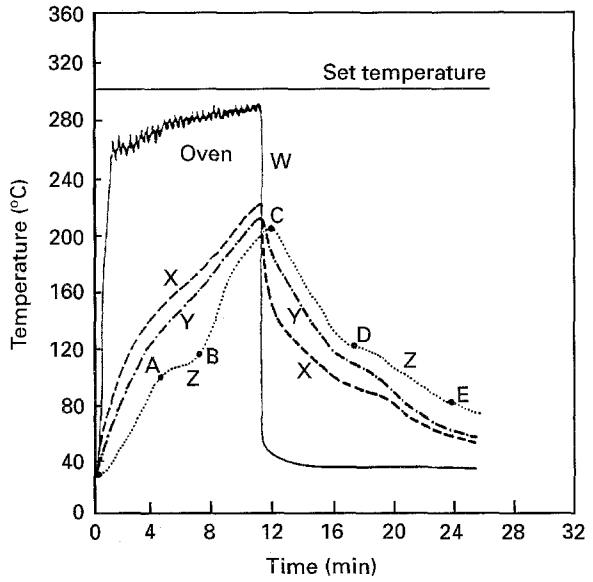

Figure 2 Rotolog trace showing oven, mould and internal temperature throughout the moulding cycle. X, outside the mould; y, inside the mould; z, air inside the mould.

error methods to achieve products of acceptable quality.

During the process the plastic undergoes a complex series of movements and phase changes as the mould rotates. With injection moulding and extrusion it is possible to monitor the melt condition throughout the cycle using thermocouples and transducers to measure temperature and pressure. In rotational moulding, the biaxial rotation of the mould makes such measurements extremely difficult. Hence, until recently, it had not been possible to identify in a precise manner when the powder had melted inside the mould or when it had reached an optimum state of curve.

However, recent research [9] has shown that if the temperature of the gas inside the mould is monitored throughout the cycle then all the key stages in the process are apparent to the machine operator and the need for trial and error is removed completely. Fig. 2 illustrates all the information relevant to a typical rotational moulding cycle. In this example, the oven set temperature is 300 °C. Normally this would be the only temperature control variable available to the machine operator. It may be seen that in the vast majority of cases this is of little value, because the oven and certainly the mould never achieve the set temperature. Curves X and Y illustrate the temperature rise on the outside and inside surfaces of the metal mould. As would be expected, the inside surface lags behind the outside surface during the heating and cooling phases.

As indicated above, however, the crucial information is contained in the inner air temperature measurement – curve Z [13]. Initially the internal air heats up relatively slowly. During this phase, the powder is tumbling about inside the mould but the temperature of the internal surface of the mould is below the "tacky temperature" at which particles of powder will start to stick to it. At point A, about $4\frac{1}{2}$ min into the cycle, the powder starts to melt and stick to the mould. As this phase change absorbs much of the thermal energy being put into the system, the internal air temperature rises less quickly over the region AB. At point B, however, all the powder has gone and there is a coating of melt on the inside surface of the mould. The energy input is therefore directed back to heating the air inside the mould and so its temperature can be seen to rise more steeply again over the section BC of the curve.

When the mould is removed from the oven (at about 11 min) the oven and mould temperatures drop almost instantaneously but the inner air temperature continues to rise for a short period. This thermal overshoot can be important in thick-wall products because it could be in the region of 10–25 °C for a period of several minutes. As will be shown later, this can have a major effect on product quality.

In the initial stages of the cooling (region CD) the cooling rate will depend on whether forced air or water spray is used. At point D the rate of decrease of inner air temperature becomes less, because solidification of the plastic is taking place and this releases thermal energy. Once the plastic as solidified, the inner air cools more quickly again and indeed it is then feasible to use much faster cooling, e.g. water spray. At point E (inner air temperature 80 °C) the mould has become sufficiently cool that it can be handled and so the product can be ejected.

The inner air temperature profile, therefore, provides all the key information to control the cycle and it makes product quality independent of oven efficiently, ambient conditions, mould material, oven setting, amount of material in the mould, etc. As far as the mechanical properties of the end-product are concerned, the peak internal air temperature (point C) has a fundamental role. In normal circumstances, air will be inside the mould throughout the cycle and although the temperature of the plastic at its inner surface will be less than it is at its outer surface (in contact with the mould), it is the inner surface which is likely to suffer degradation due to the presence of the air. Therefore, all other things being equal, there will be a correlation between peak internal air temperature and the properties of the end-product. Fig. 3 illustrates the relationship between oven time and impact strength of rotationally moulded polyethylene (Sclair 8405). In this case the oven temperature was the

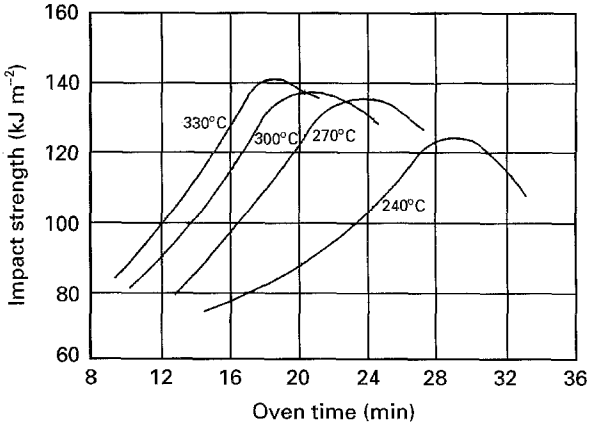

Figure 3 Effect of oven time on impact strength (from [14]).

control parameter [14]. Subsequent tests and the results reported here show that it is possible to rationalize these data by using the inner air temperature. In previous work with polyethylene, it has been found that, irrespective of all other variables, if the inner air temperature is not permitted to exceed about 200 °C, then thermal/oxidative degradation can be avoided and impact strength of the moulded product will be high. The main thrust of this paper will be to illustrate how the microstructure of the material is changing in this critical stage of the processing cycle.

4. Experimental procedure

In this investigation polyethylene powder from Enichem (RP 246 H), stabilized by the supplier with 0.04% Irganox 1010 was used as the standard material. For two sets of mouldings this powder was modified by dry blending with 0.1% and 1% antioxidant.

The mouldings, approximately 3 mm thick, were produced in a CACCIA 1400 A shuttle-type rotational moulding machine. This has a 1.6 m × 1.6 m × 1.4 m oven heated by a 7700 kcal h^{-1} liquid petroleum gas burner. The heating periods in the oven were in the range of 10–26 min at a set temperature of 300 °C. Cooling was by air fan. The mould was a cube shaped box of 440 mm × 440 mm at the top, 400 mm in height and 400 mm × 400 mm at the base, manufactured from sheet steel. The atmosphere inside the mould was air, except for one set of mouldings when nitrogen was used. The moulding conditions of the samples are shown in Table I.

TABLE I Processing conditions of rotationally moulded samples (oven temperature 300 °C)

Sample identification	Antioxidant level (%)	Atmosphere	Maximum inner temperature (°C)
S-177	0.04	Air	177
S-181			181
S-192			192
S-209			209
S-224			224
S-239			239
S-241			241
S-253			253
01-194	0.1		194
01-214			214
01-230			230
01-247			247
01-261			261
1-182	1		182
1-204			204
1-215			215
1-236			236
1-244			244
1-252			252
1-261			261
N_2-185	0.04	Nitrogen	185
N_2-207			207
N_2-222			222
N_2-233			233
N_2-241			241
N_2-256			256
N_2-265			265

In the following sections, the mouldings are identified using the alphanumeric code X-123 where X is either S for mouldings using the standard material, 01 for the material with 0.1% antioxidant, 1 for the material with 1% antioxidant or N_2 for mouldings using a nitrogen atmosphere. The next three numbers correspond to the maximum temperature reached by the air inside the mould during the processing cycle. Thus, for example, 1-204 corresponds to a moulding produced from material with 0.1% antioxidant which reached an inner air temperature of 204 °C during moulding.

The impact tests were conducted on a Rosand IFW 5 falling weight machine using a test temperature of −20 °C and impact speed of 3 m s^{-1}. The impact striker was fully instrumented to record force and displacement throughout the cycle. The fracture process was recorded with a NAC HSV-1000 FPS colour high-speed video camera enabling the recording at a speed of 1000 frames per second. A minimum of six specimens was cut either from whole mouldings or from parts where the inner layer had been previously machined away to a depth of about 0.2 mm.

The shavings obtained during the machining away of the inside layer were used to measure the material melt flow index, MFI, according to ASTM 1238.

The morphological analysis was performed on cross-sections (10–15 μm thick) with an Olympus BH2 polarizing microscope. The melting and crystallizing behaviour of the moulded material was studied in sections immersed in silicone oil, using a Mettler FP 82 hot stage fitted to the microscope.

Fluorescence microscopy was used to analyse the degradation of the samples. It was performed with an Olympus BH2 fluorescence microscope fitted with a Leitz MPV photometer. The fluorescence intensity was measured from 30 μm thick cross-sections immersed in glycerol using a 40 mm × 6 mm measuring aperture in the photometer.

The examination of the inside surface of the mouldings was done with a Leica S 360 scanning electron microscope.

Fourier transform–infrared (FHR) microscopy was performed on cross-sections microtomed parallel to the inside surface of the mouldings with a Bruker IFS 66V spectroscope.

5. Results and discussion

The micrographs obtained using polarized light microscopy revealed that the morphology of the mouldings changes according to the maximum temperature reached by the atmosphere inside the mould (inner temperature). When this temperature is too low, bubbles remain trapped within the samples (see Fig. 4 and Table II). Bubble-free samples were obtained only when the inner temperature was raised above a certain value. It was observed that this temperature was higher for mouldings prepared with a nitrogen atmosphere or from material with a higher content of antioxidant.

Under the polarizing microscope, it was observed that the general crystalline texture of the samples

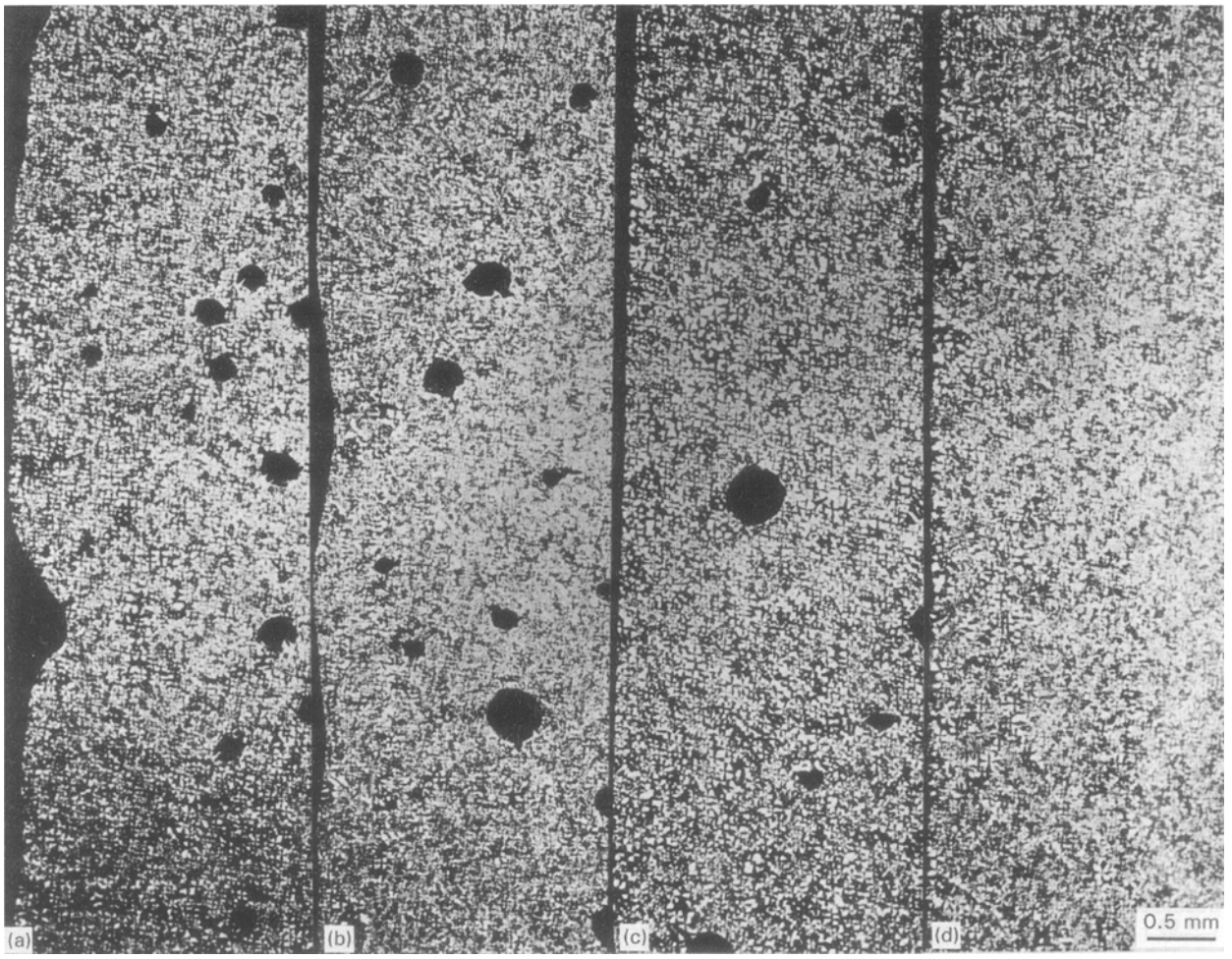

Figure 4 General views of cross-sections of samples moulded with standard material in contact with air, using a polarizing microscope. (a) Sample S-177, (b) sample S-181, (c) sample S-209, (d) sample S-239.

TABLE II Types of morphologies formed in the mouldings

Sample identification	Morphology	
	Bulk	Inside surface
S-177 to S-209	Spherulitic with bubbles	Spherulitic, very rough, with gaps
S-224	Spherulitic with small number of bubbles	Spherulitic, flat
S-239 and S-241	Spherulitic without bubbles	Very small and imperfect spherulites, very flat
S-253	Spherulitic without bubbles	Non-spherulitic, smooth surface
01-194 to 01-230	Spherulitic with bubbles	Spherulitic, very rough, with gaps
01-247	Spherulitic without bubbles	Very small and imperfect spherulites, very flat
01-261	Spherulitic without bubbles	Non-spherulitic, smooth surface
1-182 to 1-236	Spherulitic with bubbles	Spherulitic, very rough, with gaps
1-244 and 1-252	Spherulitic without bubbles	Spherulitic, rough
1-261	Spherulitic without bubbles	Mix of smooth and spherulitic patches
N_2-185 to N_2-233	Spherulitic with bubbles	Spherulitic, very rough, with gaps
N_2-241	Spherulitic without bubbles	Spherulitic, rough
N_2-256	Spherulitic without bubbles	Very small and imperfect spherulites, very flat
N_2-265	Spherulitic without bubbles	Non-spherulitic, smooth surface

consists of rather coarse spherulites with well-defined Maltese crosses and regularly spaced dark bands, these features being typical of polyethylene [15–18]. At the inside surface, the crystallization of the polymer undergoes noticeable modifications as the inner temperature increases. This is illustrated in Figs 5 and 6 showing the cross-sections and the surfaces, respectively, of mouldings heated to different inner temperatures. In mouldings processed at lower temperatures, the texture in the bulk remains apparently unchanged up to the inside surface (Figs 5a, 6a and 6b). The spherulites, grown freely from nuclei located at the

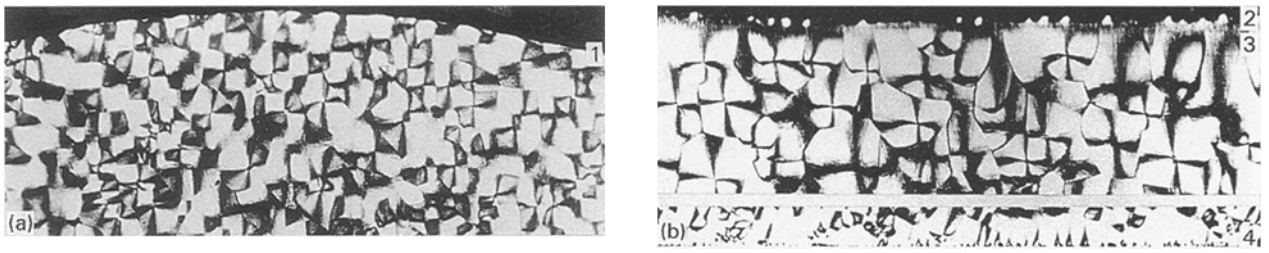

Figure 5 Polarizing micrographs showing the effect of the inner temperature on the morphology of the inside skin zone. (a) Sample S-209, (b) sample S-241, (c) sample S-253. 1, Inside surface; 2, layer of imperfect spherulites; 3, layer of columnar structures; 4, transcrystalline texture at the outer surface; 5, non-spherulitic layer.

surface, define a rough texture with deep gaps between the spherulite boundaries, as shown by the SEM examples in Fig. 6. The banded structure of the spherulites (illustrated in Fig. 7) was observed again at the inner surface of samples produced at lower inner temperatures. All the samples displayed a transcrystalline layer at the surface that contacted the mould wall (Fig. 5b).

It is apparent that when the inner temperature rises above a certain value, modifications occur in the morphology of the inside surface. When this surface is heated up to a moderately high temperature (about 240 °C for the case of the standard material moulded with an air atmosphere), the overall coarse spherulitic texture (Fig. 5a) near the inside surface is modified to a thin layer of small and imperfect spherulites (Fig. 5b). If the heating of that surface is too severe, a ribbon of non-spherulitic, low-birefringence material is formed there (Fig. 5c). In both cases, adjacent to the inside surface skin, a columnar type structure made of bundles of parallel fibrils appears, growing from the interior spherulites towards the surface as shown in regions 3 of Fig. 5b and c.

An increase in the concentration of antioxidant and the use of a nitrogen atmosphere do not prevent the above morphologies from being formed at the inside surface. However, the temperature at which they occur is raised as is indicated in Table II. This effect is apparent when Fig. 5b is compared with Fig. 8: both correspond to samples moulded at the same inner air

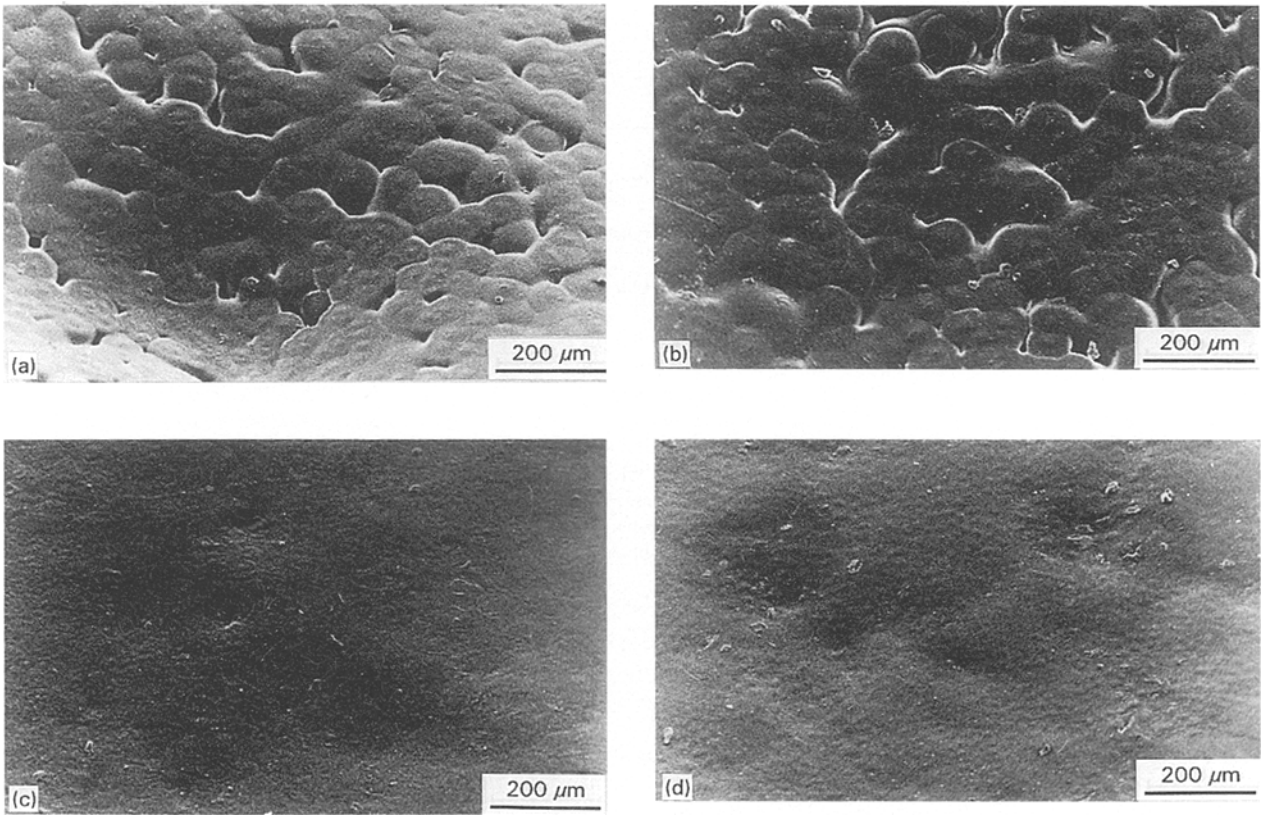

Figure 6 Scanning electron micrographs showing the effect of the inner temperature on the texture of the inside surface. (a) Sample S-177, (b) sample S-224, (c) sample S-241, (d) sample S-253.

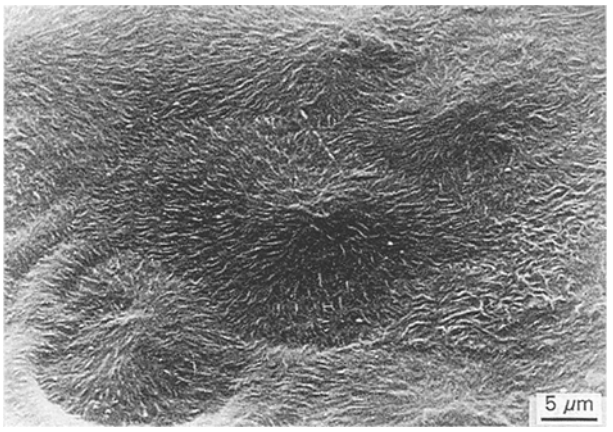

Figure 7 Spherulites nucleated at the inside surface and displaying a banded structure as seen by SEM on sample S-181.

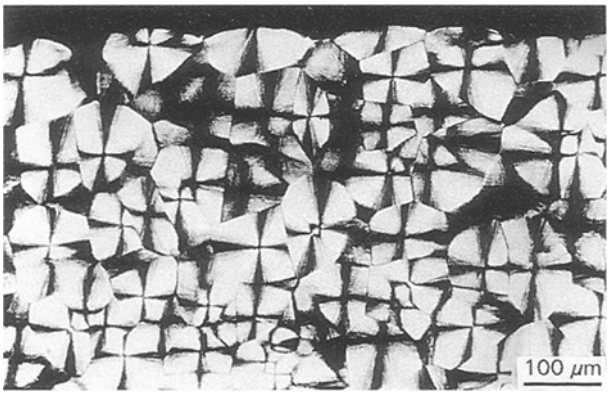

Figure 8 Polarizing micrograph of sample N_2-241 showing the spherulitic texture of the inside surface.

temperature of 241 °C, using atmospheres of air and nitrogen, respectively. Whereas in the sample processed with air, the spherulitic structure has clearly deteriorated, the one moulded with nitrogen remained apparently unaffected.

The samples made from material with a higher level of antioxidant also experienced similar structural modifications at the inside surface (as indicated in Table II and shown in Fig. 9). However, for the material with 1% antioxidant, the morphological modifications at the inside surface are not continuous along the surface but occur in discrete patches as can be observed in Figs 9c and 10.

Fluorescence microscopy, which enables the detection of double bonds in the polymer chains [19], showed that fluorescence of the inside surface only occurred where the normal spherulitic texture was altered. The fluorescence pattern does not seem to be affected by the atmosphere at the interior of the mould nor by the antioxidant level, except when the latter was very high (ca. 1%). In this case, the fluorescence is localized at rather deep and small patches (Fig. 9d) instead of being distributed over a continuous layer as illustrated in Fig. 9b for a material with 0.1% antioxidant.

In all the samples that showed fluorescence, the intensity of the emitted radiation decays rapidly with the distance from the surface and disappears where the normal spherulitic texture is reached. This behaviour is illustrated in Figs 11 and 12.

The melting behaviour of the inside wall region is closely related to the microstructure. The samples with a normal spherulitic structure up to the inside surface, melt almost uniformly throughout the thickness at about 126 °C, whereas the samples with the layered and partially non-spherulitic morphology show a discrete melt behaviour at this zone. In some cases the melting starts at the inner surface layer at 100 °C, or even below, and as the temperature rises it progresses inwards up to the normal spherulitic zone. This behaviour is illustrated in Fig. 13 for a sample with a non-spherulitic layer at the inside surface. The non-spherulitic inside surface layer and the adjacent columnar texture recrystallized in a rather similar form when cooled from 150 °C at a rate of 1 °C min^{-1}.

The FT–IR spectroscopy analysis showed that the chemical structure of the polymer suffered modifications when the samples were heated more severely. Carbonyl, vinyl and hydroperoxide groups, that are commonly produced during the oxidative degradation of polyethylene [20–22] can be identified at the inside skin layer of those samples. Fig. 14 shows two typical spectra obtained from the sample S-253. Spectrum (a) corresponds to a section cut at the inside surface and spectrum (b) was taken from a section cut further away at the spherulitic zone. The FT–IR results agreed with the fluorescence observations in that the oxidation is apparently confined to the inside skin zone.

The carbonyl region at the degraded skin of the samples produced with different additive concentrations or in the presence of nitrogen is shown in Fig. 15. Except for the case of the sample with the higher antioxidant content, all the spectra are very similar, revealing identical functional groups at this region.

The MFI data in Table III show that this parameter decreases with the increasing processing temperature. However, this decrease only occurs at the inside skin zone. The values obtained for the layer removed from the inside surface are plotted in Fig. 16. Although the thickness of the removed layers was not exactly the same for every sample, it is evident that the decrement of the MFI is a function of the maximum inner temperature. It is also clear from these results that the concentration of antioxidant and the type of atmosphere have an influence on the temperature threshold where the MFI starts to decrease more rapidly.

The impact tests at −20 °C showed that the impact strength is very sensitive to the maximum inner air temperature. As shown in Table IV and plotted in Fig. 17, the impact strength increases with the inner air temperature up to the MFI temperature threshold, and then falls sharply when this optimum temperature is exceeded.

At the test temperature of −20 °C, all the samples failed in a brittle manner except those processed at the optimum inner air temperature. The removal of the inside skin modifies the impact behaviour as shown in Table IV and Fig. 18. The samples with bubbles, resulting from processing at an inner air temperature below the optimum, showed an impact strength lower

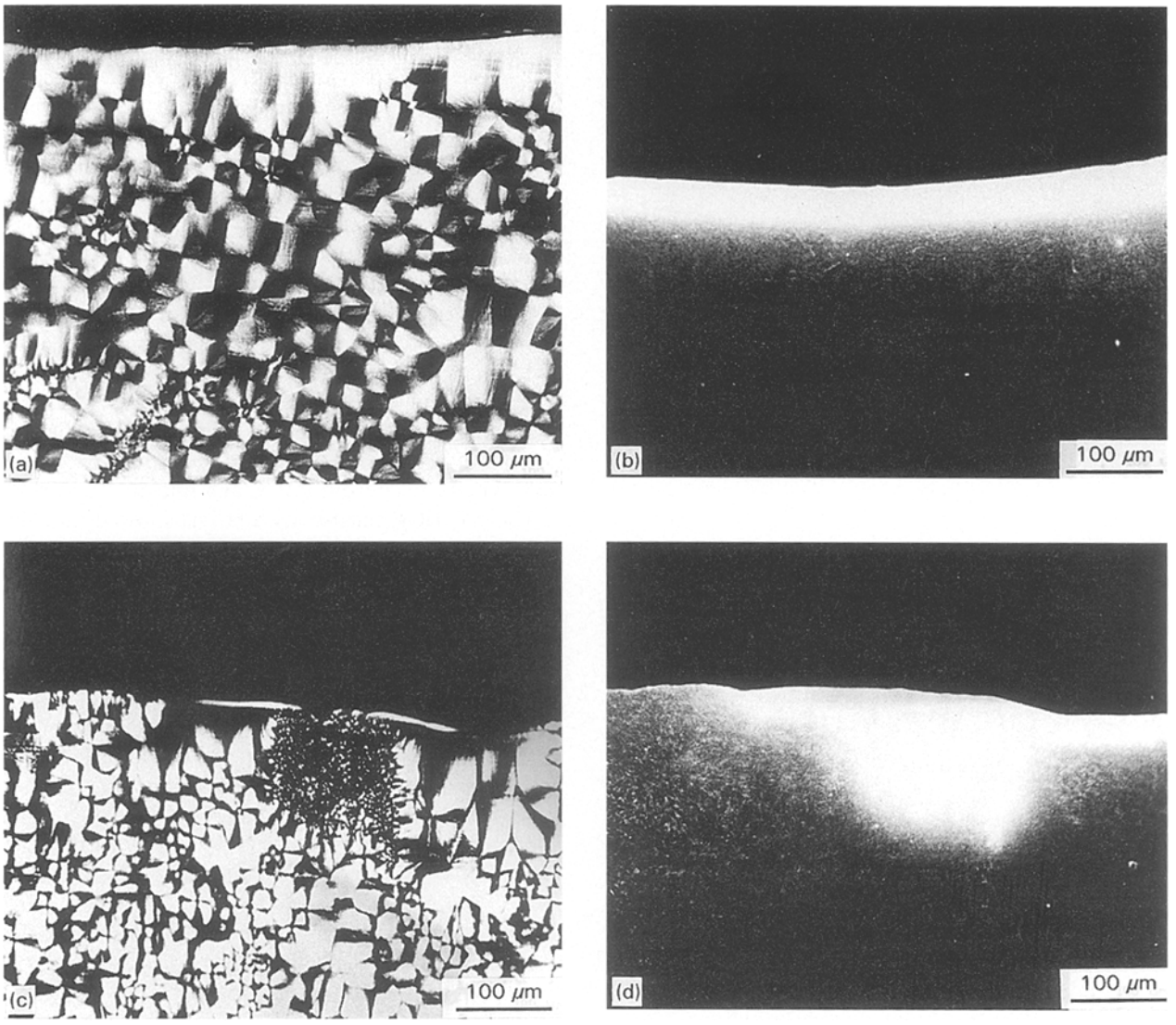

Figure 9 Micrographs showing the effect of the antioxidant concentration on the microstructure and on the fluorescence behaviour. (a) Sample 01-261 (polarized light), (b) sample 01-261 (fluorescence), (c) sample 1-261 (polarized light), (d) sample 1-261 (fluorescence).

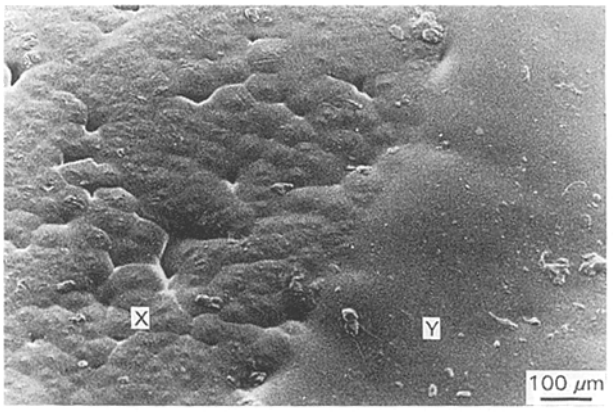

Figure 10 Scanning electron micrograph of the inside surface of sample 1-261, showing the spherulitic zone (X) and the smooth zone (Y).

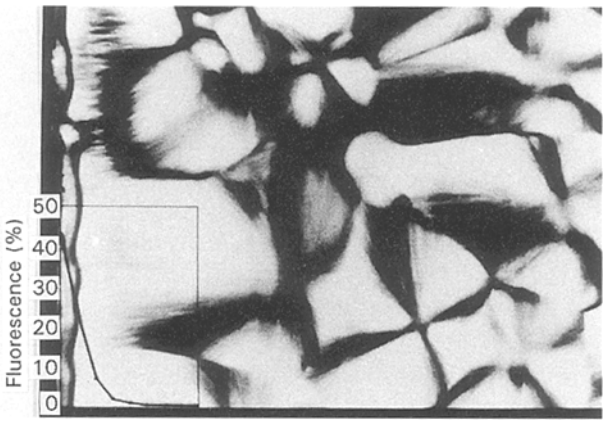

Figure 11 Plot of the variation of fluorescence intensity with the distance from the inside surface of sample S-253, superimposed upon the corresponding polarized light micrograph. (see Fig. 12 axes for details).

than when they were tested intact; these samples became even weaker upon removal of the inside skin. The high-speed video photographs show a more brittle failure when the inside skin is absent as is illustrated in Fig. 19a and b. Although the appearance of the fracture surface is identical for the specimens tested either intact or without the inside skin, in the latter, failure occurred sooner (at 2 ms after impact instead of 4 ms).

The fracture behaviour of the samples with a degraded inside skin improved noticeably upon removal

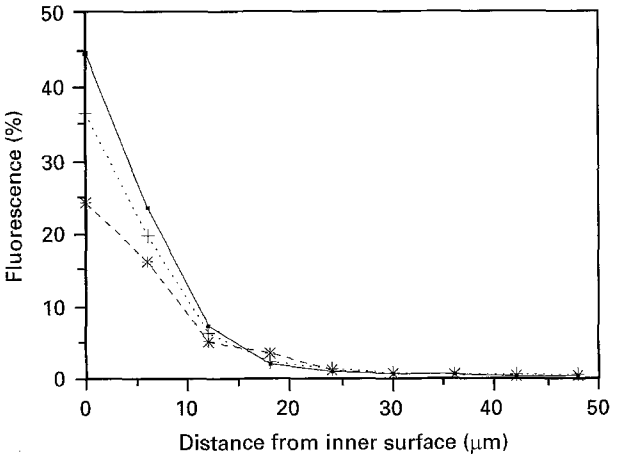

Figure 12 Plot of the fluorescence intensity measured at the inside surface of samples (■) S-253, (+) 01-261 and (*) N_2-265.

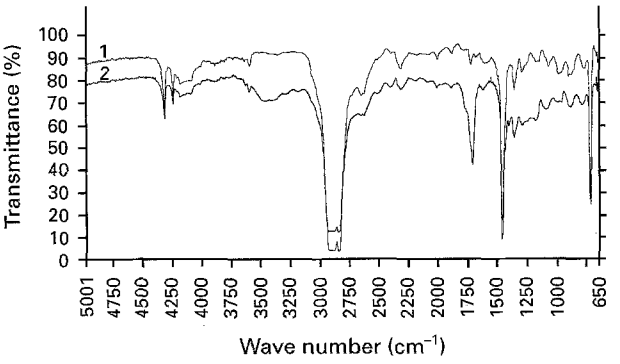

Figure 14 FT–IR spectra of sample S-253 taken at a section cut in the bulk (1) and at the inside surface (2).

of this layer. This is illustrated in Fig. 19c and d that correspond to a sample moulded with air and an inner temperature of 253 °C, from standard material, and tested either intact or without the inside skin, respectively.

5.1. Effect of degradation on morphology and properties

The degradation of the polymer, as observed in this study, is very likely to occur at temperatures not very far from the usual processing conditions. Degradation was evident from the decrease of MFI, and the occurrence of oxidized structures and of unsaturations, commonly detected in thermally oxidized polyethylene [20–23]. In particular, the carbonyl groups absorbance bands occurring at about 1720 cm^{-1} at the inside skin of samples heated up to higher temperatures is a clear indication that oxidative reactions took place. These reactions were not totally eliminated by the use of nitrogen instead of air, probably because some residual oxygen is always present, due to air being trapped in, for example, small pockets on the surface of the particles.

The increase of antioxidant concentration delayed the oxidative degradation that was shifted to higher temperatures. The radical chain reactions that take place when polyethylene is thermally oxidized are inhibited in the presence of Irganox [23–25]. However, they are not eliminated completely especially when the temperature or the heating time increase. At high melt temperatures, the Irganox efficiency as an inhibitor is therefore limited, this effect being more pronounced by agglomeration, migration to the surface, and the volatilization effects that are likely to occur. When the distribution of antioxidant is not homogeneous, local deterioration of the polymer takes place [20]. This was observed in the samples

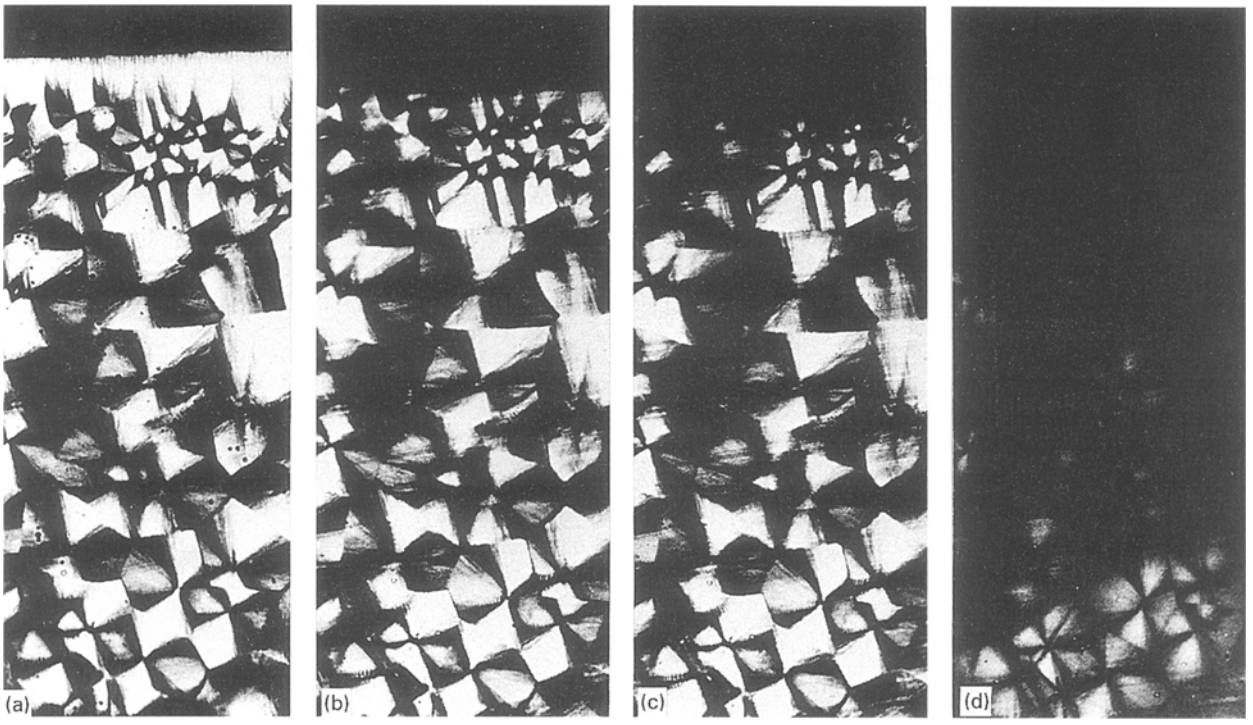

Figure 13 Cross-sections of the sample N_2-265 viewed with polarized light while being heated in the hot-stage at temperatures of (a) 75 °C, (b) 121 °C, (c) 122.5 °C and (d) 124.7 °C.

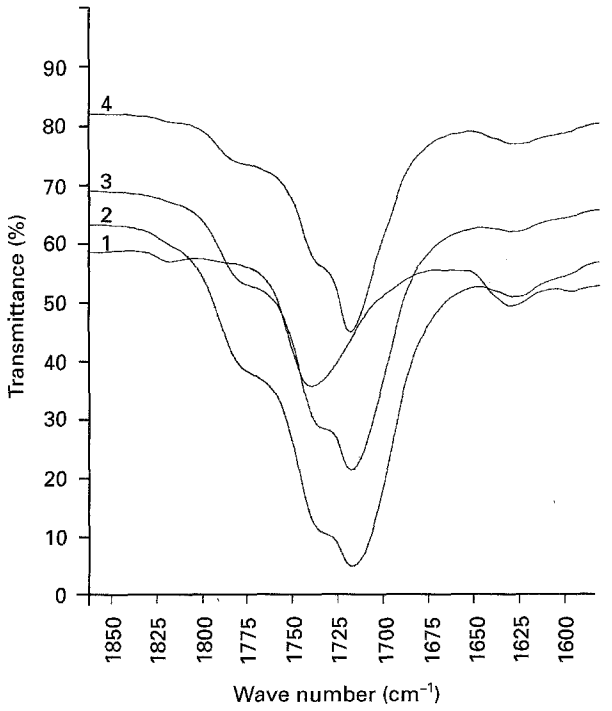

Figure 15 FT–IR spectra showing the carbonyl zones of the inside surfaces of: 1, Sample 1-261; 2, sample S-253; 3, sample 01-261; 4, sample N_2-265.

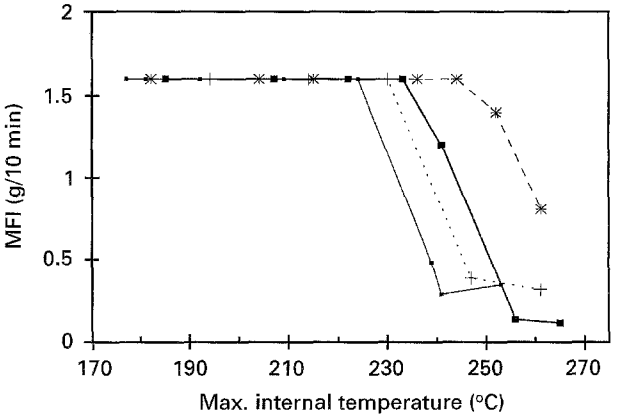

Figure 16 Effect of the inner temperature on the MFI of the inside layer of the mouldings. (■) 0.04% Irg., (+) 0.1% Irg., (*) 1% Irg., (■) N_2.

with the highest content of Irganox which were processed at 261 °C and showed deeply degraded zones surrounded by regions where degradation was apparently inhibited.

In the degradation of polyethylene, chain scission and chain branching leading to cross-linking occur simultaneously as competitive reactions. During fabrication processing cross-linking typically predominates [22–25] and this is likely to be the case for rotational moulding as was clearly depicted by the decreasing MFI reported here and elsewhere [14]. The decrease of the MFI is more noticeable when the mould is filled with nitrogen, because by reducing the availability of oxygen, intermolecular recombination leading to an increase of molecular weight is favoured [20].

Under the fluorescence microscope, the double bonds of the carbonyl and the vinyl groups, build up during the degradation of the polymer, fluoresce under irradiation in the ultraviolet region. The π-electrons of these bonds, which are less strongly held than the σ-bonding electrons, absorb radiation in the ultraviolet region and emit light within the visible spectrum range, thus making the specimens exhibit fluorescence. This technique was previously used to study the degree of degradation of PVC [19]. In this study it was shown to be particularly helpful for determining the extent of the degradation across the thickness and to relate this to the modifications in the morphology.

The sharp decay of the fluorescence intensity with distance from the inside surface confirms that the oxidative reactions occurring there are controlled by the diffusion rate of oxygen (Table V). In such situations, as the oxidative reactions develop, the difficulty of carrying oxygen through to maintain them results in a decrease of the oxygen concentration. Consequently, the degradation rate also decreases with the increasing distance from the surface [26].

The crystallization behaviour of the polymer was shown to be strongly affected by the extent of degradation. In the absence of degradation (which is apparent

TABLE III MFI results

Sample identification	MFI (g/10 min) (inside layer)	MFI (g/10 min) (sample with inside layer removed)	Sample identification	MFI (g/10 min) (inside layer)	MFI (g/10 min) (sample with inner layer removed)
S-177	1.6	1.8	1-182	1.6	1.8
S-181	1.6	1.8	1-204	1.6	1.8
S-192	1.6	1.8	1-215	1.6	1.8
S-209	1.6	1.8	1-236	1.6	1.8
S-224	1.6	1.8	1-244	1.6	1.8
S-239	0.48	1.8	1-252	1.4	1.8
S-241	0.29	1.8	1-261	0.81	1.8
S-253	0.35	1.8			
01-194	1.6	1.8	N_2-185	1.6	1.8
01-214	1.6	1.8	N_2-207	1.6	1.8
01-230	1.6	1.8	N_2-222	1.6	1.8
01-247	0.39	1.8	N_2-233	1.6	1.8
01-261	0.32	1.8	N_2-241	1.2	1.8
			N_2-256	0.14	1.8
			N_2-265	0.12	1.8

TABLE IV(a) Low temperature (− 20 °C) impact test results, through complete wall section and with inside layer removed

Sample identification	Impact strength of intact sample (J)	Impact strength of sample with inside layer removed (J)	Sample identification	Impact strength of intact sample (J)	Impact strength of sample with inside layer removed (J)
S-177	2.02 (1.4)[a]	7.0 (1.8)	1-182	7.6 (1.2)	5.5 (1.1)
S-181	10.0 (1.8)	5.8 (0.9)	1-204	9.9 (1.9)	7.0 (1.2)
S-192	12.2 (1.4)	7.6 (0.8)	1-215	10.8 (2.3)	9.5 (1.1)
S-209	14.2 (1.0)	8.5 (1.9)	1-236	16.2 (0.7)	14.7 (4.9)
S-224	18.1 (1.0)	21.4 (2.8)	1-244	15.6 (1.3)	19.3 (2.0)
S-239	7.7 (2.4)	20.2 (1.3)	1-252	7.5 (2.0)	20.3 (1.4)
S-241	5.4 (0.7)	20.8 (1.7)	1-261	6.9 (3.0)	18.8 (0.9)
S-253	7.2 (1.2)	20.1 (3.6)			
01-194	11.8 (0.9)	8.2 (2.2)	N_2-185	12.2 (1.6)	7.3 (3.4)
01-214	12.5 (1.0)	8.2 (3.0)	N_2-207	14.0 (1.0)	9.8 (1.3)
01-230	18.2 (1.3)	21.7 (2.3)	N_2-222	16.3 (1.2)	17.0 (1.2)
01-247	5.8 (0.8)	22.8 (1.4)	N_2-233	18.0 (0.9)	20.3 (1.5)
01-261	6.4 (0.9)	21.4 (1.7)	N_2-241	18.7 (1.2)	20.5 (1.5)
			N_2-256	8.7 (1.1)	16.1 (3.1)
			N_2-265	7.4 (1.5)	19.6 (2.6)

[a]Numbers in parentheses are standard deviations.

TABLE IV(b) Low temperature (− 20 °C) impact test results, through complete wall section and with inside layer removed

Sample identification	Impact strength of intact sample ($J\,mm^{-1}$)	Impact strength of sample with inside layer removed ($J\,mm^{-1}$)	Sample identification	Impact strength of intact sample ($J\,mm^{-1}$)	Impact strength of sample with inside layer removed ($J\,mm^{-1}$)
S-177	2.0 (0.4)[a]	1.8 (0.4)	I-182	1.9 (0.3)	1.5 (0.3)
S-181	2.6 (0.4)	1.5 (0.2)	1-204	2.5 (0.5)	1.9 (0.3)
S-192	3.0 (0.3)	2.0 (0.5)	1-215	2.8 (0.6)	2.5 (0.3)
S-209	3.5 (0.2)	2.2 (0.5)	1-236	4.3 (0.2)	4.0 (1.3)
S-224	4.6 (0.2)	5.8 (0.7)	1-244	4.3 (0.3)	5.5 (0.4)
S-239	2.1 (0.7)	5.8 (0.3)	1-252	2.0 (0.5)	5.4 (0.7)
S-241	1.4 (0.2)	5.5 (0.2)	1-261	1.8 (0.8)	5.5 (0.2)
S-253	1.9 (0.3)	5.9 (0.8)			
01-194	2.9 (0.2)	2.1 (0.6)	N_2-185	3.0 (0.4)	2.0 (0.9)
01-214	3.2 (0.3)	2.1 (0.7)	N_2-207	3.6 (0.2)	2.6 (0.4)
01-230	4.8 (0.2)	6.1 (0.4)	N_2-222	4.2 (0.3)	4.8 (0.3)
01-247	1.5 (0.2)	6.0 (0.2)	N_2-233	4.7 (0.2)	5.5 (0.4)
01-261	1.7 (0.2)	5.9 (0.4)	N_2-241	4.9 (0.2)	5.7 (0.3)
			N_2-256	2.3 (0.2)	5.0 (0.4)
			N_2-265	1.9 (0.4)	5.4 (0.6)

[a]Numbers in parentheses are standard deviations.

from either the absence of fluorescence and carbonyl groups, or by the unchanged MFI), the polymer crystallized to produce its normal spherulitic morphology which is widely described in the literature, e.g. [15–18]. The nucleation and growth of this type of texture throughout the thickness was identical at all points and gave rise to structures of similar shape and size.

In the degraded samples (as in Fig. 5b and 5c) the spherulitic structure was severely altered. These modifications of the microstructure took place alongside a decrease of the melting point, this being an indication that the perfection of the crystalline structure decreased. Similar observations were made by Terselius *et al.* [27, 28] at the inside wall of oxidized polyethylene pipes. The microstructural modifications observed in this work were probably caused by the increase in the molecular weight of the polymer due to cross-linking. According to Maxfield and Mandelkern [29], the molecular weight has a strong effect on the supermolecular structure of linear polyethylene. These authors showed that when molecular weight increases, the resulting spherulites display a high degree of imperfection. They also reported that the addition of a small amount of a high molecular weight fraction to a spherulitic forming pool causes a major decrease in the spherulite size, and that further addition leads to the complete loss of structure. However, the increase in molecular weight does not seem to be the only cause for the deterioration of the crystalline texture of the polymer. The study of Scheirs *et al.* [30] on thermal oxidation of polyethylene powder reported the decrease of the molecular weight, but with a deterioration of the structure also taking place. Thus it appears that both the molecular weight increase and the presence of irregularities in the polymer chain contribute to the modifications of the crystalline texture observed in this study.

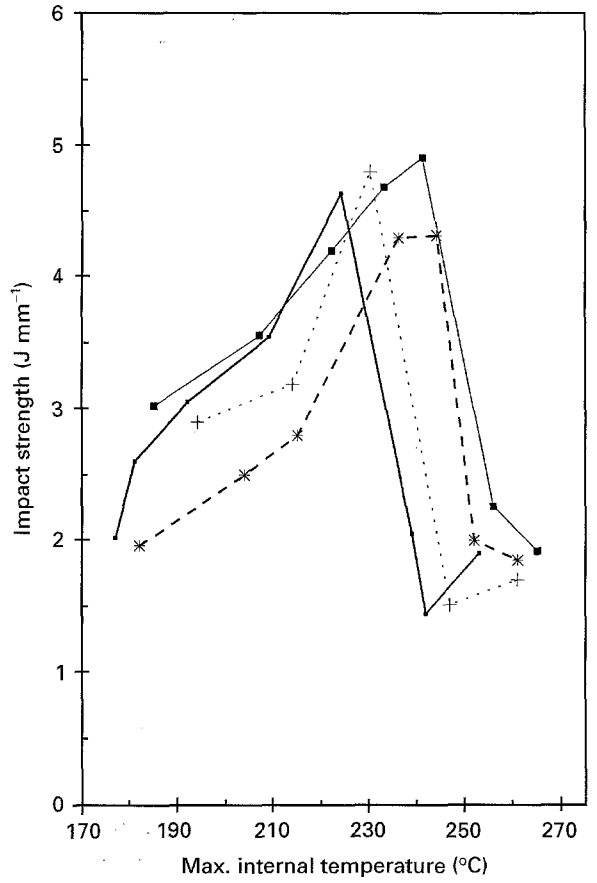

Figure 17 Effect of the maximum internal temperature (inner temperature) on the impact strength of the mouldings. (■) 0.04% Irg., (+) 0.1% Irg., (*) 1% Irg., (■) N_2.

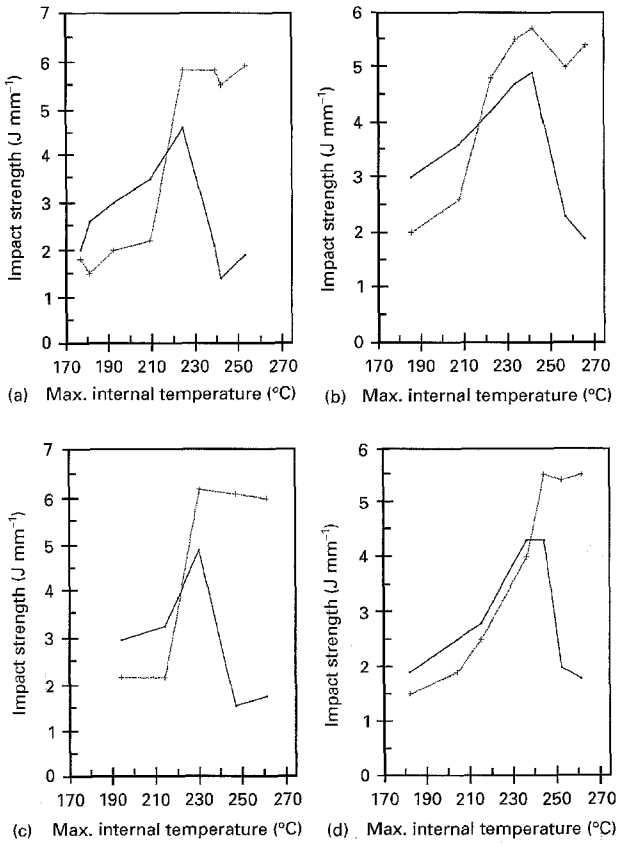

Figure 18 Effect of the removal of the inner layer on the impact strength of the mouldings. (a) Standard conditions, (b) nitrogen atmosphere, (c) 0.1% antioxidant, (d) 1% antioxidant. ■) Intact, (+) without inner layer.

The detrimental effect of the removal of the inside skin in the samples with bubbles is explained by the stress concentration effect that the bubbles have when they are left uncovered at the surface by the machining operation.

The increase of the impact strength when the degraded skin is removed confirms that the degradation is restricted to the inside surface, and the properties of the material in the bulk are almost unaffected by the processing temperature provided that no bubbles are left there. This is illustrated in Fig. 19.

The lower impact strength of the samples moulded with 1% antioxidant is probably due to the excessive concentration of the additive. Padrón *et al.* [31] observed a similar loss in tensile properties when high concentrations of antioxidant were used, this being explained primarily by the decrease in the solubility of the additives.

6. Conclusions

In this work the morphology of rotationally moulded polyethylene has been related to the processing conditions and in this way the variations which occur in mechanical properties, such as impact strength, can be explained. The following main conclusions have been drawn.

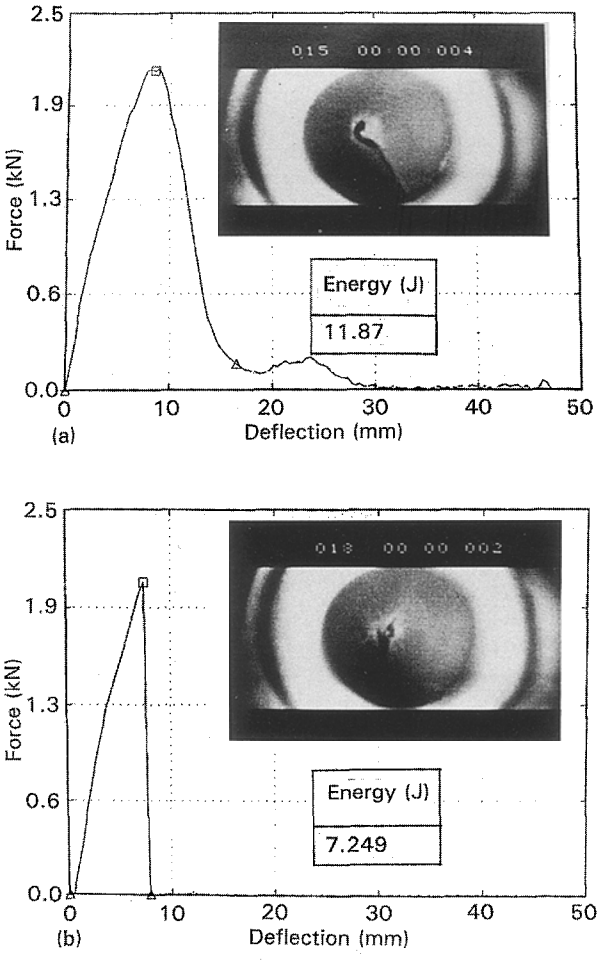

Figure 19 High-speed video pictures of the impact failure and corresponding force–deflection diagram of the tests. (a) Intact sample (S-215), (b) sample with the inside layer machined away (S-215), (c) intact sample (S-253), (d) sample with the inside layer machined away (S-253).

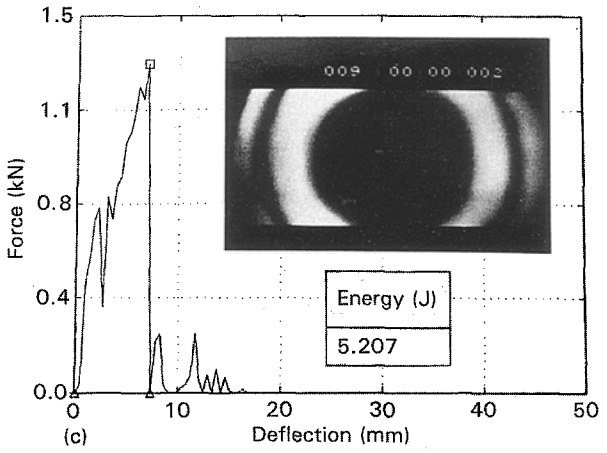

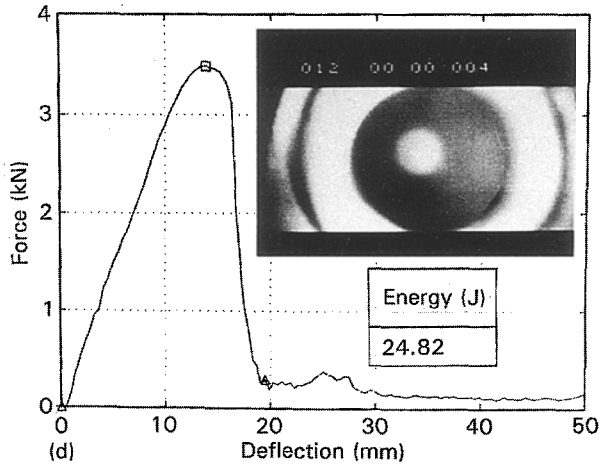

Figure 19 continued

1. The impact strength of rotationally moulded polyethylene is very sensitive to the value of internal atmosphere temperature achieved during the moulding cycle.

2. At low internal temperatures the impact strength is low, due to incomplete sintering of the powder particles. This is accompanied by pin-holes within the structure of the polymer. At high internal temperatures the impact strength is reduced due to a degraded layer which forms on the inner free surface of the moulding.

3. In slightly overheated mouldings there is a thin layer of imperfect spherulites at the inner surface and next to it is a columnar-type structure consisting of bundles of parallel fibrils. When a greater amount of overheating occurs, the columnar structure is preceded by a thin layer of non-spherulitic material at the free surface.

4. In all cases there is a transcrystalline layer at the surface in contact with the mould. There was no evidence that this reduced impact strength.

5. The degradation of the inner surface of rotationally moulded polyethylene products is predominantly due to a cross-linking of the structure.

6. The use of increased amounts of antioxidant in the polymer or the use of an inert atmosphere delays the degradation process but does not prevent it.

7. There is no evidence of degradation within the wall thickness of the mouldings, even when there is an excessive amount of overheating.

TABLE V Fluorescence measurements

S-239		S-253		N_2-256		N_2-265		01-247		01-261		1-252		1-261	
Distance from inside surface (μm)	Fluor. (%)	Distance from inside surface (μm)	Fluor. (%)	Distance from inside surface (μm)	Fluor. (%)	Distance from inside surface (μm)	Fluor. (%)	Distance from inside surface (μm)	Fluor. (%)	Distance from inside surface (μm)	Fluor. (%)	Distance from inside surface (μm)	Fluor. (%)	Distance from inside surface (μm)	Fluor. (%)
0	1.9	0	44.7	0	18.8	0	24.4	0	6.9	0	36.6	0	30.1	0	34.5
6	1.3	6	23.7	6	10.8	6	16.2	6	6.1	6	19.8	6	16.5	6	24.8
12	0.8	12	7.3	12	5.1	12	5.1	12	2.0	12	6.3	12	6.0	12	10.8
18	0.4	18	2.1	18	1.6	18	3.6	18	0.8	18	2.4	18	3.5	18	5.9
24	0.3	24	1.1	24	0.8	24	1.3	24	0.4	24	1.5	24	2.4	24	3.7
30	0.3	30	0.8	30	0.4	30	0.8	30	0.4	30	0.9	30	1.6	30	2.8
		36	0.7	36	0.4	36	0.7	36		36	0.8	36	1.3	36	2.3
		42	0.5	42		42	0.5	42		42	0.7	42	1.2	42	1.9
		48	0.5	48		48	0.5	48		48	0.7	48	1.2	48	1.7
														54	1.6
														60	1.5
														66	1.3
														72	1.3

8. The removal of the degraded layer at the inside surface of rotomoulded products results in full recovery of the impact strength of the material.

Acknowledgements

The authors thank Enichem for the supply of polyethylene for this work. The work was made possible by a grant from the British Council to facilitate travel between laboratories.

References

1. M. A. RAO and J. L. THRONE, *Principles of Rotational Moulding*, **12**(4) (1972) 237.
2. P. F. BRUINS, "Basic Principles of Rotational Moulding" (Gordon and Breach, New York, 1971).
3. J. JACKSON, *Engineering*, **2** February (1989) 63.
4. K. IWAKURA, Y. OHTA, C. H. CHEN and J. L. WHITE, *Int. Polym. Proc.* **IV** (1989) 2.
5. P. J. NUGENT, PhD thesis, Queen's University, Belfast (1990).
6. J. A. SCOTT, PhD thesis, Queen's University, Belfast (1986).
7. R. J. CRAWFORD, "Rotational Moulding of Plastics" (Research Studies Press, Wiley, Chichester, 1992).
8. *Idem, Prog. Rubb. Plast. Technol.* **6**(1) (1990) 1.
9. R. J. CRAWFORD and P. J. NUGENT, *Plast. Rubb. Compos. Proc. Appl.* **17** (1992) 23.
10. *Idem, ibid.* **11** (1989) 107.
11. P. J. NUGENT, R. J. CRAWFORD and L. XU, *Adv. Polym. Technol.* **11**(3) (1992) 181.
12. D. W. SUN and R. J. CRAWFORD, *Polym. Eng. Sci.* **33** (1993) 132.
13. R. J. CRAWFORD and P. J. NUGENT, US Pat. 5322654, Eur. Pat. PCT/GB 90/01569, 1990.
14. *Idem, Plast. Rubb. Compos. Proc. Appl.* **17** (1992) 33.
15. D. C. BASSET, "Principles of Polymer Morphology" (Cambridge University Press, Cambridge, 1981).
16. A. S. VAUGHAN and D. C. BASSET, in "Comprehensive Polymer Science", Vol 2, Polymer Properties, edited by G. Allen and J. C. Bevington (Pergamon, London, 1989).
17. D. C. BASSET, *ibid.*
18. A. KELLER, *Plast. Rubb. Proc. Appl.* **4** (1984) 85–92.
19. D. A. HEMSLEY, R. P. HIGGS and A. MIADONYE, *Polym. Commun.* **24** (1983) 103.
20. M. IRING and F. TÜDÓS, *Prog. Polym. Sci.* **15** (1990) 217.
21. M. IRING, T. K. LÁSZLÓ-HEDVIG, F. TÜDÓS, L. FÜZES, G. SAMAY and G. BODOR, *J. Polym. Sci. Symp.* **57** (1976) 55.
22. H. HINSKEN, S. MOSS, J.-R. PAUQUET and H. ZWEIFEL, *Polym. Degrad. Stability* **34** (1991) 279.
23. S. MOSS and H. ZWEIFEL, *ibid.* **25** (1989) 217.
24. R. T. JOHNSTON, in "Advances in the Stabilization and Controlled Degradation of Polymers", edited by A. V. Pastis (1986) pp. 169–81.
25. F. MITTERHOFER, *Polym. Eng. Sci.* **20** (1980) 692.
26. A. J. C. PADRÓN, M. A. COLMENARES, Z. RUBINZTAIN and L. A. ALBORNOZ, *Eur. Polym. J.* **23** (1987) 723.
27. B. TERSELIUS, U. W. GEDDE and J.-F. JANSSON, *Polym. Eng. Sci.* **23** (1982) 422.
28. U. W. GEDDE, J.-F. JANSSON and B. TERSELIUS, *ibid.* **27** (1987) 727.
29. J. MAXFIELD and L. MANDELKERN, *Macromolecules* **10** (1977) 1141.
30. J. SCHEIRS, S. W. BIGGER and O. DELATYCHI, *J. Polym. Sci. Polym. Phys.* **29** (1991) 795.
31. A. J.C. PADRÓN

Received 20 September
and accepted 25 October 1995